MPPT of Solar Energy Conversion System with Modified Perturb and Observe Algorithm Using Bisection Method

Akanksha Singh S. Vardhan[1,*] and Rakesh Saxena[1]

ARTICLEINFO

Article history:
Received: 14 June 2021
Revised: 2 September 2021
Accepted: 15 September 2021

Keywords:
Renewable energy sources
Maximum power point tracking
Perturb and observe algorithm
MATLAB Simulink
Bisection approach Agro residues based power plant

ABSTRACT

This study proposes a modified perturb and observe algorithm-based maximum power point tracking (MPPT) for solar energy conversion systems using the bisection method. There is a huge demand for electricity at every level of life in the twenty-first century. Traditional energy sources like coal, diesel, and gasoline, as well as nonconventional energy sources like hydro, solar, and wind, are used to meet these power needs. The problem with non-renewable energy sources is that they pollute the environment, contributing to climate change through the greenhouse effect, and they are also non-reusable. As a result, to overcome these challenges, we use renewable energy sources. Renewable energy sources, on the other hand, have a problem with efficiency. The purpose of this study is to discuss photovoltaic MPPT, which is used to extract the greatest power from the sun's energy. The perturb and observe methodology was changed in this work to use the bisection technique, which delivers quicker and better results than the standard perturb and observe method. In addition, the recommended approach is verified using MATLAB Simulink.

1. INTRODUCTION

A photovoltaic system consists of a solar array, battery, charge controller, DC/DC Boost Converter, inverter, voltage sensor, current sensor, and variable resistors [1]. This solar array generates photocurrent and photovoltage when exposed to sunlight [2-4]. The Current and Voltage sensors detect photocurrent and photovoltage, respectively. Batteries store energy so that it may be delivered even when there is no light [5-6]. Deep discharge batteries are required in solar PV applications. In deep discharge batteries, the maximum depth of discharge allowed should be at least 80% [7]. Plate wrap is prevented by making the electrode plates thicker and more durable. Thicker plates are linked with larger active material and, as a result, better charge capacity [8-10]. Figure 1 depicts the location of the MPPT algorithm as well as duty cycle adjustment in a PV system.

There are two reasons for using the battery in solar PV system:

1. There is no sun insolation throughout the night. As a result, if a load requires electricity at night, the battery, which is charged during the day, provides it.
2. It may not be possible to use all of the energy provided by the PV source in a stand-alone system. The most often used batteries in PV systems are lead-acid and nickel-cadmium batteries. Charge controllers are used to minimise deep draining or overcharging in order to ensure maximum performance and battery life. To convert the DC voltage level, the DC-to-DC converters are connected. A network of storage components like as capacitors and inductors, as well as power devices such as diodes and transistors, is used to achieve this energy shift. Figure 2 shows the PV array generating electricity, storing it in a battery, and transmitting it to the load.

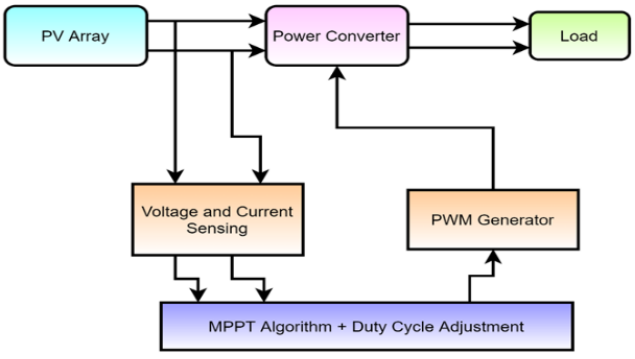

Fig. 1. MPPT algorithm for PV system.

[1]*Department of Electrical Engineering, Shri G.S. Institute of Technology & Science, Indore, India*.
**Corresponding author:* Akanksha Singh S. Vardhan; E-mail: Phone: +91-7080469923, E-mail: aakankshasingh843@gmail.com.

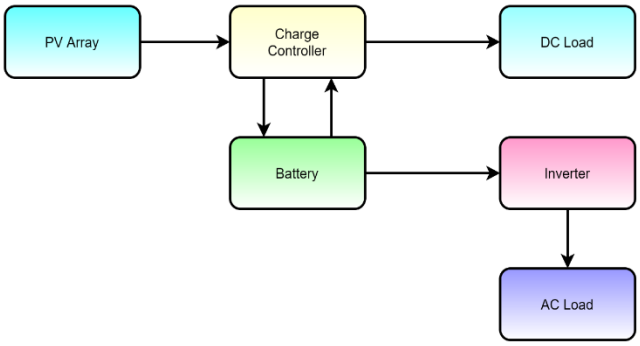

Fig. 2. Overall system configuration for PV system.

2. EFFECT OF DIFFERENT PARAMETERS

The photocurrent is generated by moment irradiation. At this point, the irradiation is proportional to the current output. Despite the fact that the irradiation may drop or raise as indicated in Figure 3, the voltage will keep a reasonably constant value and will not fluctuate considerably.

2.1 Temperature Effect on Photovoltaic Current

The open circuit voltage lowers as the temperature rises, reducing the solar cell's efficiency. Finally, despite a little increase in density, the current density will account for any increased temperature sensitivity, as illustrated in Figure 4.

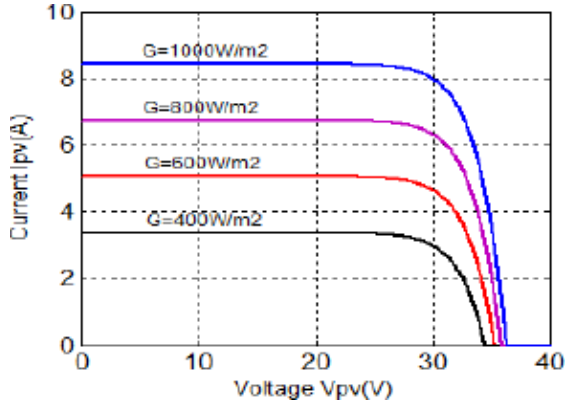

Fig. 3. Effect of irradiance on PV current.

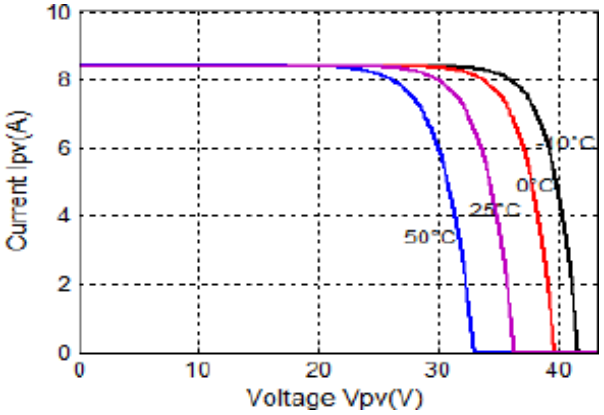

Fig. 4. Effect of temperature on PV current.

2.2 Effect of irradiance on photovoltaic power

The influence of irradiation variation at constant temperature on determining the maximum MP point is crucial, as illustrated in Figure 5. The photovoltaic module will provide the primary MPP.

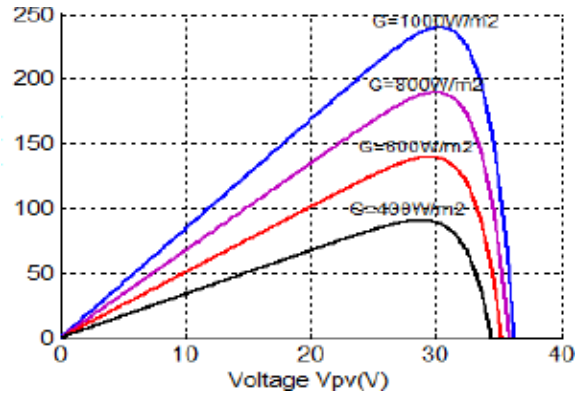

Fig. 5. Effect of irradiance on PV power.

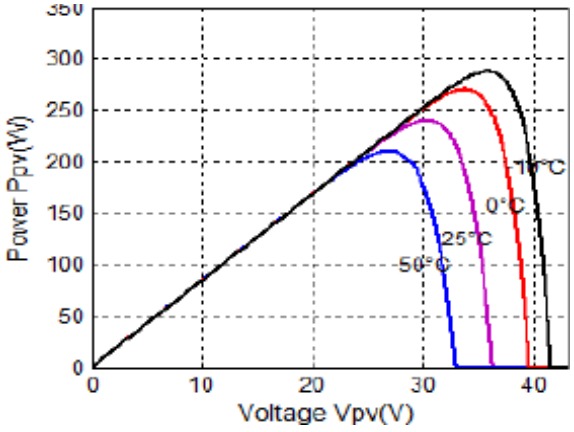

Fig. 6. Effect of temperature on PV power.

As demonstrated in Figure 6, the voltage is inversely proportional to the influence of temperature. Until a specific value is achieved, this voltage maintains a nearly linear power. The capacity of this facility decreases as the temperature rises. Finally, when the temperature rises, so does the output power and terminal voltage. The facility generated by the panel diminishes as the temperature rises, despite the fact that the panel receives the best irradiation around midday.

3. PERTURB AND OBSERVE ALGORITHM FOR MPPT

The efficiency of PV plants improves as the value of the generated power rises. The cost of power generated will be reduced due to important factors. A PV system's efficiency is primarily determined by three elements [11-13]. The first is the efficiency (commercial PV panels have an efficiency of 8-18%), the second is the inverter efficiency (usually 95–

98%), and the third is the MPPT algorithm efficiency (which has approximately 98 percent efficiency). It is extremely difficult to enhance the efficiency of PV panels and inverters. It is contingent on the availability of contemporary technology; it necessitates the use of higher-quality power electronics components, which may raise installation costs. It is easier and less expensive to update the MPPT using new control algorithms [14-16, 20-21]. That's possible to do it in plants that already have updated control algorithms in place. It might result in an immediate boost in PV power output and, eventually, a cost decrease.

Because of the nonlinear voltage-current characteristic of PV arrays, MPPT algorithms play a significant role. It has a single spot where the most power is generated. The MP point is determined by the irradiance and temperature of the panel. During the day, both conditions alter, and they also fluctuate based on yearly seasonal fluctuations. Furthermore, irradiation changes fast owing to changes in meteorological conditions such as clouds. In practise, it is a basic necessity to track the MPP precisely under all potential climatic conditions, ensuring that the PV system always obtains the maximum available power [17-19, 22-23].

3.1 Proposed Methodology and Algorithm

Because of their low number of required measurable parameters and simple structure, perturb and observe (P&O) algorithms are extensively used for MPPT control approach. As the name says, the notion behind this approach is based on the monitoring of PV array output power and its disruption by adjusting the voltage of the PV array's current during operation. The method constantly decrements or increases the reference current or voltage based on past power levels until it achieves the MPP. The MPPT algorithm in this technique is based on calculating PV power and measuring power change by sampling PV voltage and current.

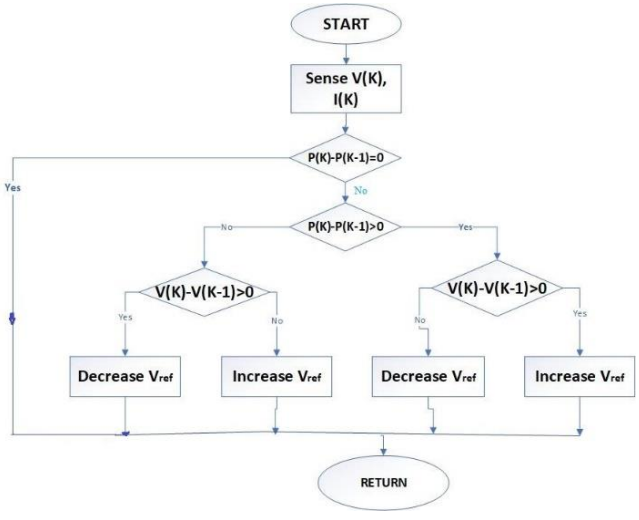

Fig. 7. Flow chart of the proposed perturb and observe method.

The proposed method is shown in the Figure 7. When the PV array's operating voltage is disturbed in the experiment's prescribed direction and the dP/dV<0 is less than one, the operating point is moved away from the MP point. The suggested P&O method shifts the perturbation's direction. If dP/dV>0 during the experiment, the PV array would be pushed towards the MPP at that moment due to a change in operating point. At this time, the P&O algorithm is still perturbing the PV array's voltage in the same direction. This style is known as hill climbing methodology because of its nature. Because of its reliance on power increases versus voltages above and below the MPP.

3.2 Modified perturb and observe algorithm based on Bisection method

This approach is most useful when using the PV array's immediate voltage and current. In this technique, sampling takes place once every switching cycle. This method was continued until the MPP was reached. The PV system is oscillating near the planned MPP at this time. The output oscillation of the system was reduced when the perturbation step size was reduced. However, when the amount of the disturbance is reduced, the MPPT may decelerate down.

In this study, a variation to the traditional P&O method is suggested. The MP operational point is achieved earlier in this modified P&O technique than in the regular P&O method. First, the voltage is monitored, and then a power calculation is offered to be performed at any time. After examining the slope (dP/dV), the authors must examine if the operational point is placed on the left-hand side of the MPP or on the right-hand side of the MPP. For calculating the relevant power, a specified increment (say 3volts) with positive slop is supplied. The slope-checking procedure is conducted once more. The increment is kept going with positive slop. The immediate voltage and power are approximated using negative slop.

The flow chart of bisection method used in this paper is shown in Figure 8. V_{pos} is the earlier voltage with the specified positive slope that corresponds to the earlier power. Similarly, V_{neg} is the voltage that corresponds to the power of negative slope. The slope checking is recommended after calculating the average voltage of the V_{pos} and V_{neg}. The obtained power is referred to as MPP when the slop is within a certain range. To reach the average value for the next positive slope, the new average voltage V_{pos} must be updated with the previous value of V_{neg}. This technique is repeated until a very narrow range (about 0.1) is not discovered.

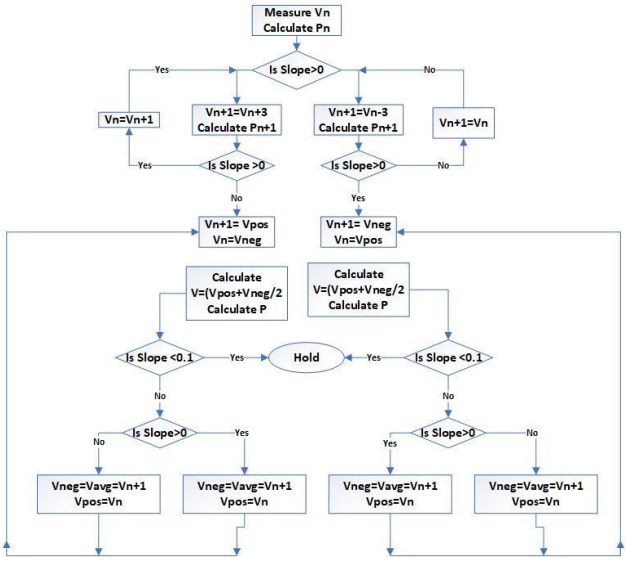

Fig. 8. Flowchart of Bisection Method.

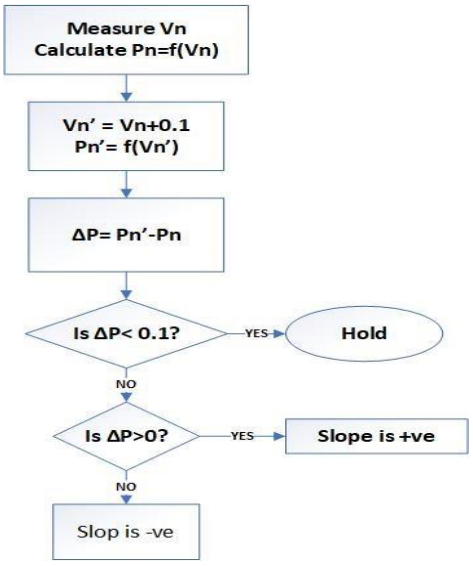

Fig. 9. Procedure for slope checking.

In the negative slope, a similar procedure is used. This voltage, which corresponds to the final power on the negative side, is updated as V_{neg} with the same value as V_{pos}. It is determined the average of the two voltages, V_{pos} and V_{neg}. MPP is to be tracked if the evaluated new average voltage appears in the given narrow range. This process is repeated until the MPP of the PV array is attained.

If the slope is negative after measuring the voltage and power, some particular decrement of voltage is done at first until the voltage reaches positive dP/dV. V_{pos} and V_{neg} denote the freshly obtained voltage at positive dP/dV and the last acquired voltage at negative dP/dV, respectively. For average voltage slope verification, the average voltage of the V_{pos} and V_{neg} must be assessed. The voltage V_{pos} has been updated for MPPT with positive slope, while the voltage V_{neg} has been updated for negative slope. This step is repeated until the average value falls inside the desired narrow range. Figure 9 depicts the flowchart of this experimental procedure. In the decision box of the algorithm, the suggested improved algorithm specifies the subroutine and operation of the PV system.

3.3 Performance Characteristics of PV System

This section depicts the performance characteristics of a PV system. Two sets of terminal voltage and circulating current readings from the PV module have been noted from the experimental setup. Table 1 shows the computed values of produced power (W), Figures 10 and 11 depict the PV array's I-V and P-V properties, respectively at starting voltage of 3V. Another value of starting voltage is taken to be 13V and the data is shown in Table 2. The I-V and P-V curves at this condition are shown in Figures 12 and 13 respectively. For simulation work, the results are derived using MATLAB using tabular data gathered from the PV module.

Table: I, V, P reading from photovoltaic module for starting voltage of 3 V

I(A)	V(V)	P(W)
0.69	0.00	0.000
0.67	2.50	1.675
0.66	4.00	2.640
0.65	5.50	3.575
0.63	8.00	5.040
0.59	10.00	5.900
0.53	11.50	6.095
0.45	13.00	5.850
0.42	13.50	5.670
0.38	14.00	5.320
0.20	15.50	3.100
0.12	16.00	1.920

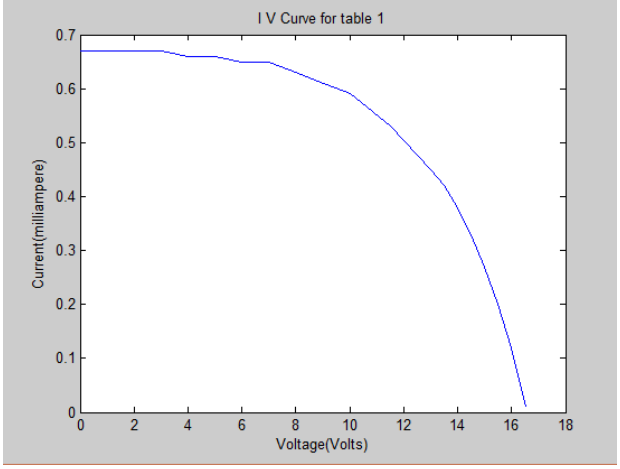

Fig. 10. I-V Curve at 3V.

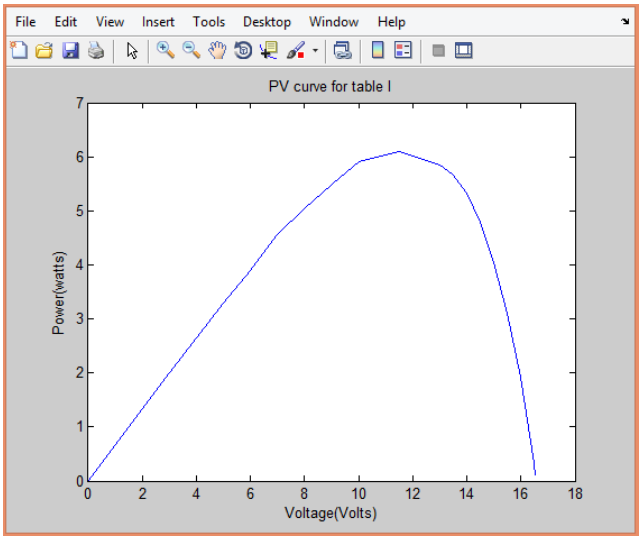

Fig. 11. P-V Curve at 3V.

Table 2: I, V, P reading from photovoltaic module for starting voltage of 13 V

I (A)	V(V)	P(W)
0.70	0.00	0.0000
0.68	0.86	0.5848
0.67	4.38	2.9346
0.66	8.09	5.3394
0.64	9.76	6.2464
0.62	12.08	7.4896
0.54	12.98	7.0092
0.42	13.99	5.8758
0.36	15.04	5.4144
0.19	15.96	3.0324
0.17	16.15	2.7455
0.00	17.95	0.0000

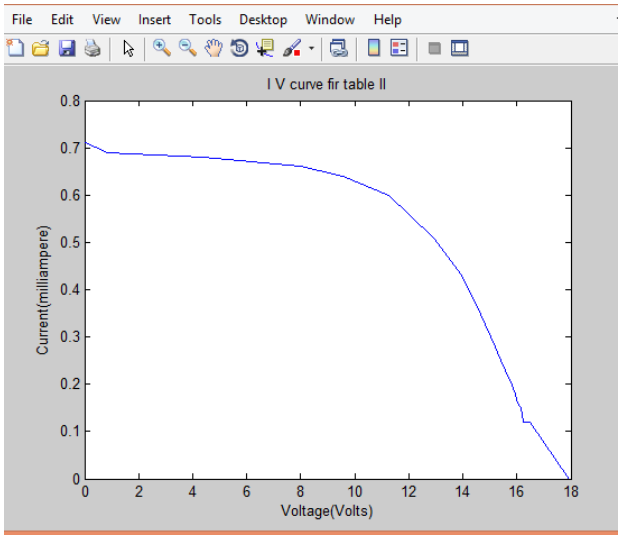

Fig. 12. I-V Curve at 13 V.

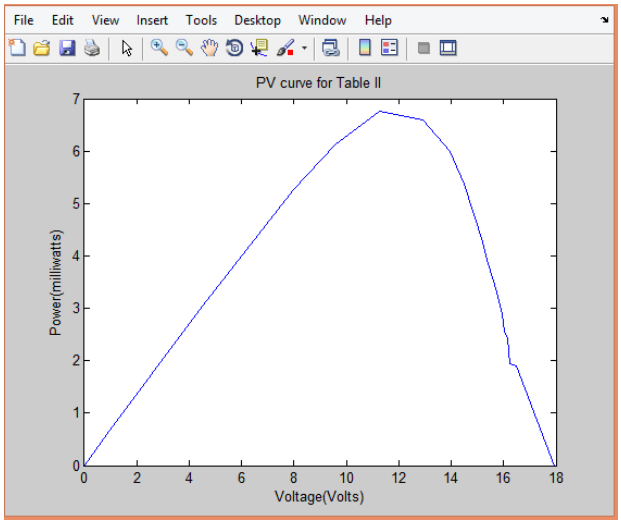

Fig. 13. P-V Curve at 13V.

4. SIMULATION ANALYSIS OF PHOTOVOLTAIC SYSTEM

This section presents a simulated study of solar system components using the suggested technique.

4.1 Simulink analysis of Iph

The equation of the I_{ph} is given in equation (1).

$$I_{ph} = I_{sc} + K_i(T_c - T_r)G \quad (1)$$

The simulation of I_{ph} is shown in Figure 14 which is done in MATLAB Simulink.

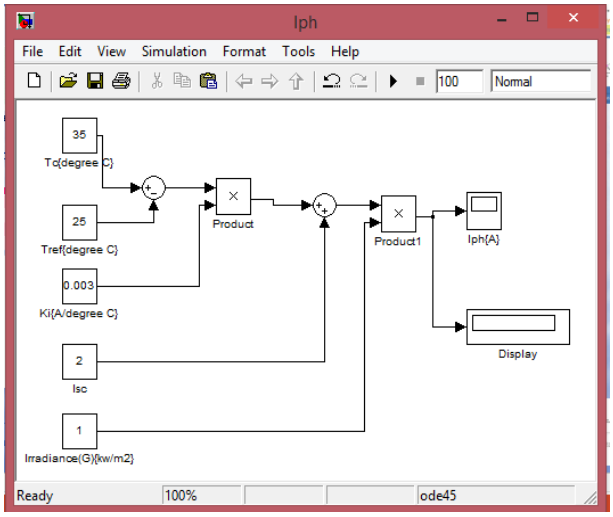

Fig. 14. Simulink model for I_{ph}.

4.2 Simulink analysis of Irs

The equation used for I_{rs} is given in equation 2.

$$I_{rs} = \frac{I_{sc}}{\left[e^{\frac{qV_{OC}}{N_S K A T_c}}\right]} - 1 \qquad (2)$$

The Simulink model is as shown in Figure 15 for I_{rs}.

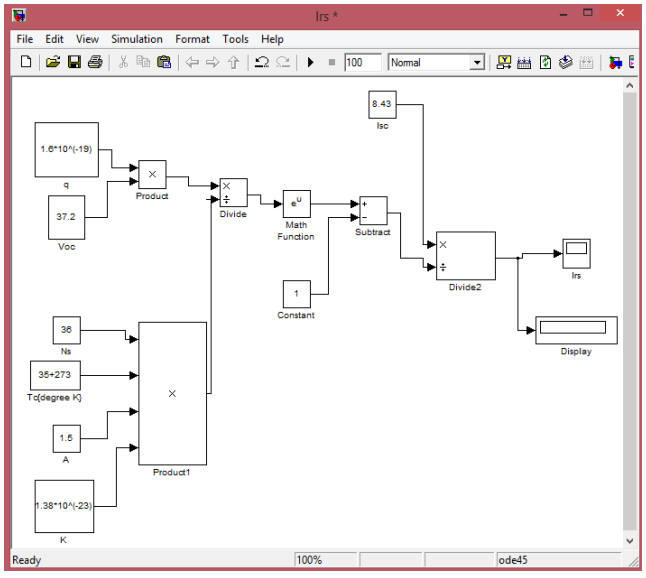

Fig. 15. Simulink model of I_{rs}

4.3 Simulink analysis of Is

The equation used for I_s is illustrated in equation 3.

$$I_s = I_{rs}\left(\frac{T_c}{T_r}\right)^3 e^{qEg\left(\frac{1}{T_r}-\frac{1}{T_c}\right)/KA} \qquad (3)$$

4.4 Simulink analysis of I_{pv}

The equation used for I_{pv} is described in equation 4.

$$I_{pv} = N_p I_{ph} - N_p I_s\left[e^{(q/KT_cA)(V_{pv}/N_s)} - 1\right] \qquad (4)$$

The Simulink models for both I_s and I_{pv} are shown in Figures 16 and 17 respectively.

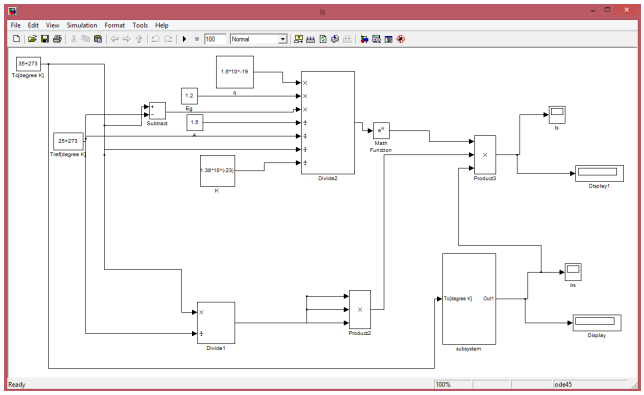

Fig. 16. Simulink model of I_s

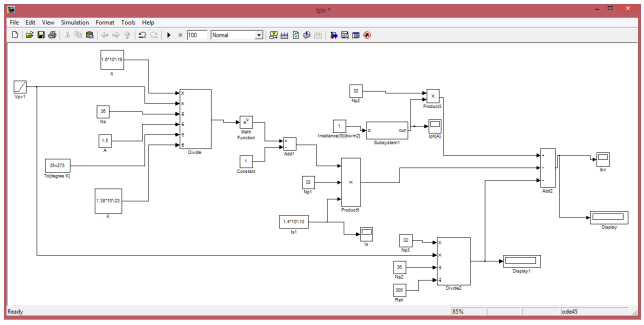

Fig. 17. Simulink model of I_{pv}

5. P-V CURVE SIMULINK MODEL OF THE PV MODULE

This section uses the user defined block to describe the PV module's Simulink model as shown in Figure 18. For table 1, the following equation is calculated using the excel function. The function to be utilized is as given in equation 5.

$$I = -0.0084V^3 + 0.1365V^2 + 0.0629V \qquad (5)$$

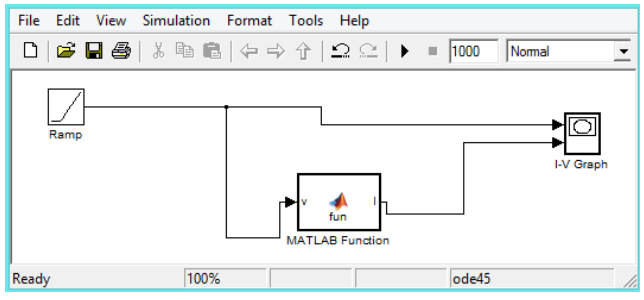

Fig. 18. P-V Curve Simulink model of the PV module.

In the experimental module, a continuous input of 3 volts is first provided via the traditional P&O approach. The associated power is then assessed and updated as old power in the following phase. The matching power is calculated

using a +0.1 increase. This computed power is updated to reflect the new voltage as a new power. Finally, the difference between two absolute power values is calculated. If the difference is greater than a defined number (in this case, 0.0005) and the old power is less than the new power, the increment procedure is repeated until the MPP is reached. During the experiment, a 0.1 decrement is applied, and the process is repeated until the absolute values of the difference of two powers exceed the specified amount of 0.0005. During this procedure, the new power must be less than the previous power for the maximum power to be considered attained. The Simulink model of the traditional perturb and observes methodology illustrates this behavior. The Simulink model for the modified P&O utilizing the bisection method combines the two approaches.

5.1 Simulink model of conventional P&O technique

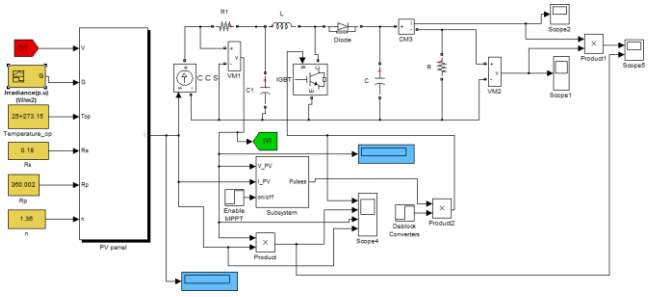

Fig. 19. Simulink model of conventional P&O technique

The Simulink model of conventional P&O technique is shown in Figure 19.

5.2 Results and Discussion

Using the function equation and the table data, the simulated I-V curve and P-V curve are created as shown in Figures 20 and 21 respectively. It has a positive constant of 0.4477 in the specified function. As indicated in the curve, the simulated P-V graph begins with this constant value. Using the mat file produces a more accurate graph.

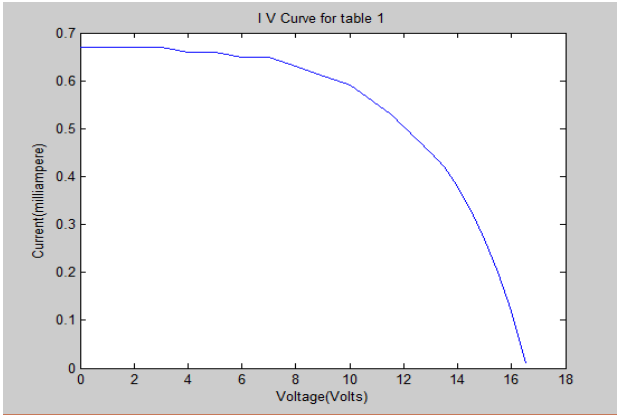

Fig. 20. I-V Curve of PV system.

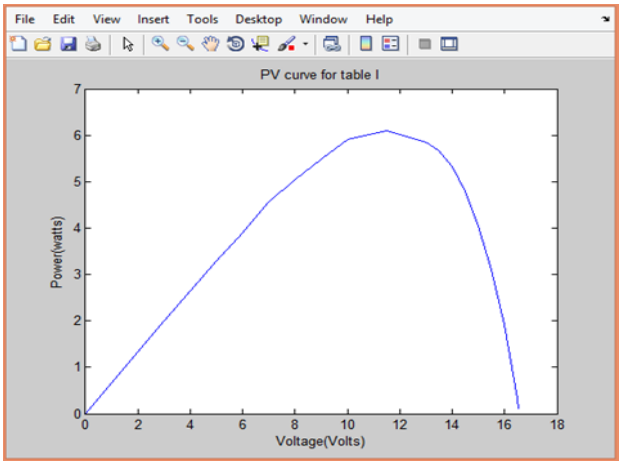

Fig. 21. P-V Curve of PV system.

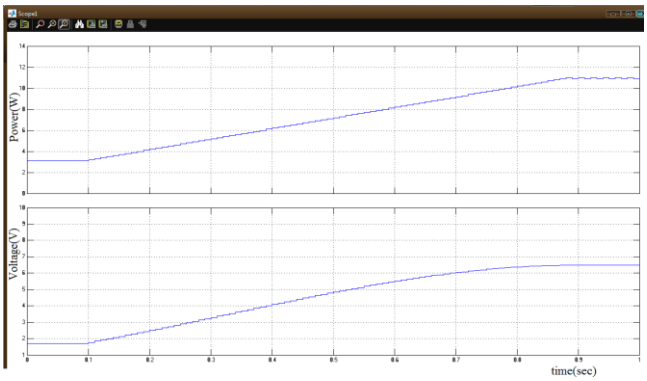

Fig. 22. V_{mpp} and P_{mpp} by conventional P&O technique for starting 3V.

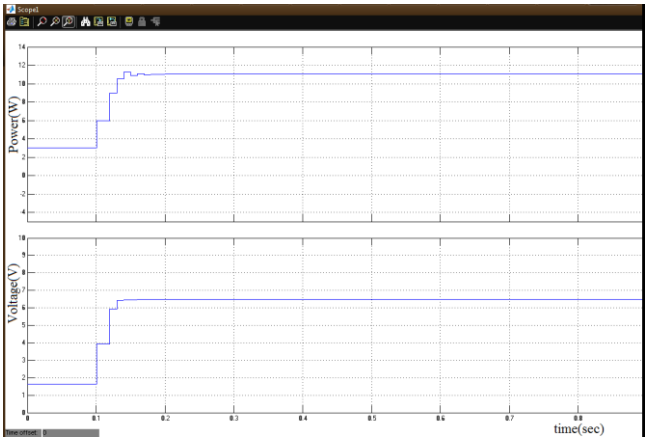

Fig. 23. V_{mpp} and P_{mpp} by Modified P&O using bisection method for starting voltage of 3V.

The graphical representations depict the simulated outcome of the traditional P&O methodology. The voltage begins to rise from the starting 3V and then achieves its maximum value, as shown by the obtained curves in Figures 22, 23 and 24. It also displays the voltage value at which the maximum power is attained in the lower curve by the V_{mpp} and P_{mpp} by Modified Perturb and Observe utilising the

bisection approach in the lower curve. The comparison of the two procedures for V_{mpp} and P_{mpp} was effectively shown. For the traditional P&O approach, a blue tint or a gently ascending curve is created in the upper. For the improved P&O approach, the graph with green colour increasing quickly to the voltage where the acquired power is maximal is explained. The modified P&O reaches the voltage at which the power is greatest faster than the conventional P&O, according to the comparison description.

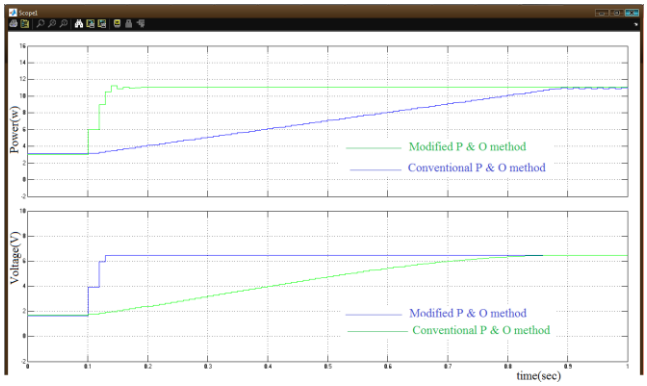

Fig. 24. V_{mpp} and P_{mpp} of combined two methods for a starting voltage of 3 volts.

Also, in the lower portion of the graph, the green curve represents the maximum power achieved by conventional P&O, while the blue curve represents the greatest power achieved by the modified P&O methodology. The updated P&O approach takes less time than the traditional P&O methodology, according to the results of the testing. The graph is produced in both situations with a starting voltage of 3 volts.

The results of the simulation were analysed using the bisection algorithm for both the traditional and developed P&O. The many input voltage levels that have been regarded as variables in the system are depicted. The Vmmp is 11.50 volts, while the PV cell's maximum output voltage is 16.52 volts, according to experiments. As a result, simulations were run with 3V as the input variable to the function, which is less than 11.50V, in order to evaluate the utilised methodology for tracking MPP. The end result reveals that the improved approach tracks the MPP significantly faster than the traditional P&O approach.

6. CONCLUSION

In this article, different MPPT methods for solar PV systems were presented. Based on the standard perturb and observe methodology, a modified perturb and observe strategy using the bisection method is developed. With this enhanced approach, the maximum power is monitored faster than with the old perturb and observe method. The entire system was modelled and simulationd using MATLAB. The simulation findings show that the new method is significantly faster at tracking maximum power than the old P&O strategy. The simulation findings show that the new method is significantly faster at tracking maximum power than the old P&O strategy. Hence, it is concluded that this technique is useful to control the MPP of PV modules since the need for renewable energy sources is increasing in the twenty-first century owing to non-endable resources and non-polluting nature.

ABBREVIATIONS

V_{PV}	Voltage of PV array
I_{PV}	Current of PV array
P_{PV}	Power output of PV array
G	Irradiation
PV	Photo-voltaic
MPPT	Maximum Power Point Tracking
I_{Ph}	Phase current
I_{sc}	Short-circuit current
I_{RS}	Reverse saturation current
V_{oc}	Open-circuit voltage
K	Boltzmann‘s constant

ACKNOWLEDGEMENT

The authors are thankful to the Department of Electrical Engineering, Shri G.S. Institute of Technology & Science, Indore (Madhya Pradesh) India for providing necessary facilities to complete this research work. The corresponding author dedicates this research work to sweet memories of her great grandfathers Baoo and Dadda for their constant support and Aashirvaad to complete my higher engineering education smoothly.

REFERENCES

[1] D.P. Kothari, I.J. Nagrath, R.K. Saket, “Modern Power System Analysis”, Fifth Edition, McGraw Hill, New Delhi, 2021.

[2] Rizwan, M, Majid Jamil and D.P. Kothari, ‘Performance Evaluation of Solar Irradiance Models: A Comparative Study’, International Journal on Electronics and Electrical Engineering, vol 1, no. 1, 141–151, 2009.

[3] Vipin Kumar, Sandip Ghosh, N.K. Swami Naidu, Shyam Kamal, R.K. Saket, S.K. Nagar (2021), “A Current Sensor Based Adaptive Step-Size MPPT With SEPIC Converter for PV Systems”, IET Renewable Power Generation (UK), In Press, 2021.

[4] Vipin Kumar, Sandip Ghosh, N.K. Swami Naidu, Shyam Kamal, R.K. Saket, S.K. Nagar (2021), “Load voltage - based MPPT technique for standalone PV systems using adaptive step”, International Journal of Electrical Power & Energy Systems, Elsevier, volume: 128, e106732, Early access 2021.

[5] Sachin Kumar, Kumari Sarita, SS Akanksha Vardhan, M Rajvikram Elavarasan, RK Saket, Narottam Das (2020),

"Reliability Assessment of Wind-Solar PV Integrated Distribution System using Electrical Loss Minimization Technique", MDPI Energies, Vol: 13, Issue: 21, pp: 01-30, 2020.

[6] Luckey Chaukse, P.A. Pattanaik and R.K. Saket (2014), "Maximum Power Point Tracking of Photovoltaic System Using Feedback Fuzzy System", IEEE International Conference on Recent Advances and Innovations in Engineering (ICRAIE-2014), May 9-11, 2014, pp: 01 – 06, 2014.

[7] A. Y. Abdelaziz, M. Ezzat, W. Sameh, R.K. Saket and Anand Kumar K.S. (2015), "An Integrated Passive Islanding Detection Method for grid Connected PV Distributed Generators", Book: Power Electronics and Renewable Energy Systems, LNEE Series, Springer Nature, pp: 131-144, 2015.

[8] Podder, A.K., et al.: MPPT methods for solar PV systems: a critical review based on tracking nature. IET Renewable Power Generation, 13(10), 1615– 1632, 2019.

[9] Shaw, P.: Modelling and analysis of an analogue MPPT-based PV battery charging system utilising dc–dc boost converter. IET Renewable Power Gener. 13(11), 1958–1967, 2019.

[10] Subudhi, B., Pradhan, R.: A comparative study on maximum power point tracking techniques for photovoltaic power systems. IEEE Trans. Sustainable Energy 4(1), 89– 98 (2013)

[11] Liu, F., et al.: A variable step sizeINC MPPT method for PV systems. IEEE Trans. Ind. Electron. 55(7), 2622– 2628, 2008.

[12] Elobaid, L.M., et al.: Artificial neural network- based photovoltaic maximum power point tracking techniques: a survey. IET Renewable Power Generation, 9(8), 1043– 1063, 2015.

[13] Kamal, T., et al.: A robust online adaptive B- spline MPPT control of three- phase grid- coupled photovoltaic systems under real partial shading condition. IEEE Trans. Energy Convers. 34(1), 202– 210, 2018.

[14] Kalla, U.K., et al.: Slide mode control of microgrid using small hydro driven single- phase seig integrated with solar pv array. IET Renewable Power Gener. 11(11), 1464– 1472, 2017.

[15] Bollipo, R.B., et al.: Critical review on PV MPPT techniques: classical, intelligent and optimisation. IET Renewable Power Gener. 14(9), 1433– 1452, 2020.

[16] Ahmed, J., Salam, Z.: A modified P&O maximum power point tracking method with reduced steady- state oscillation and improved tracking efficiency. IEEE Trans. Sustainable Energy 7(4), 1506– 1515, 2016.

[17] Ram, J.P., Rajasekar, N.: A novel flower pollination based global maximum power point method for solar maximum power point tracking. IEEE Trans. Power Electron. 32(11), 8486– 8499, 2017.

[18] Kumar B.S., Sudhakar K. (2015) Performance evaluation of 10 MW grid connected solar photovoltaic power plant in India. Energy Rep 1:184–192, 2015.

[19] Kumari Sarita, Sachin Kumar, Aanchal Singh S. Vardhan, Rajvikram Madurai Elavarasan, R.K. Saket, G.M. Shafiullah, Eklas Hossain, "Power enhancement with grid stabilization of renewable energy-based generation system using UPQC-FLC-EVA technique," IEEE Access, Vol. 8, Pages: 207443-207464 2020.

[20] Jately, Vibhu, Brian Azzopardi, Jyoti Joshi, Abhinav Sharma, and Sudha Arora. "Experimental Analysis of hill-climbing MPPT algorithms under low irradiance levels." *Renewable and Sustainable Energy Reviews* 150 (2021): 111467.

[21] Nadeem, Ahsan, and Afaq Hussain. "A comprehensive review of global maximum power point tracking algorithms for photovoltaic systems." *Energy Systems* (2021): 1-42.

[22] Osmani, Khaled, Ahmad Haddad, Thierry Lemenand, Bruno Castanier, and Mohamad Ramadan. "An investigation on maximum power extraction algorithms from PV systems with corresponding DC-DC converters." *Energy* 224 (2021): 120092.

[23] Abderrahim, Taouni, Touati Abdelwahed, and Majdoul Radouane. "Improved strategy of an MPPT based on the sliding mode control for a PV system." *International Journal of Electrical and Computer Engineering* 10, no. 3 (2020): 3074.